Self-Assembled Monolayers of Synthetic Hemoproteins on Silanized Quartz

Denis L. Pilloud,* Francesc Rabanal, Brian R. Gibney, Ramy S. Farid,† P. Leslie Dutton, and Christopher C. Moser

The Johnson Research Foundation, Department of Biochemistry and Biophysics, University of Pennsylvania, Philadelphia, Pennsylvania 19104

Received: October 15, 1997; In Final Form: January 9, 1998

To better understand the relation between structure and function of complex natural heme proteins, we have designed and synthesized de novo simplified versions called *maquettes*. Furthermore, we have assembled organized monolayers of these heme protein maquettes onto silanized quartz to more define their structural and functional properties and to take the first step in constructing robust devices that exploit biological chemistry. First, two di-α-helical peptides, α_2, were designed and synthesized to self-assemble into a four-helix bundle $[\alpha_2]_2$. The assembly has a well-developed hydrophobic interior and coordinates iron protoporphyrin IX (heme) by bis-histidine ligation. The chemisorption of these synthetic hemoproteins onto silanized quartz was achieved by reacting disulfide bridges in the loop region of each α_2 with thiols immobilized at the surface. Self-assembled monolayers of synthetic hemoproteins were characterized by UV/vis spectroscopy. UV absorption of the tryptophan reveals the presence of peptides on the substrate, and circular dichroism (CD) seems to indicate that the axes of the α-helices are oriented at a angle less than 45° relative to the substrate. The construction of monolayers of hemoproteins was successfully achieved in two different ways: (1) Hemes were incorporated after the apoproteins were self-assembled onto the silanized quartz substrate. This process led to bis-histidyl ligated hemes and to physisorbed porphyrins inside or at the surface of the monolayer. Physisorbed hemes were removed by immersion of the film in NaCl and imidazole solutions. (2) Heme-containing holoproteins were prepared in solutions before self-assembly onto silanized quartz. Linear dichroism of the heme bis-ligated to the histidines showed an average tilt angle of the porphyrin plane of 40° relative to the surface, consistent with an inclination of the whole assembly on the substrate suggested by CD measurements. Monolayers of hemoproteins, after reduction, bind CO by displacing one of the histidines. Their absorption spectra are remarkably similar to the ones reported for the cytochrome c_3.

Introduction

In contrast with small hemoproteins such as myoglobin or cytochromes, many of which are known at atomic resolution, large natural proteins associated with membranes and involved in respiration and photosynthesis are not as well characterized. In recent years, several structures of the photosynthetic reaction center[1] have been solved at high resolution, and most recently, cytochrome oxidase[2] and the cytochrome bc_1 complex[3] structures have been described. These proteins, built around multiple membrane spanning α-helices, are enormous hydrophobic structures and incorporate many elaborations that attend to biological activities divorced from the principal function of building an electrochemical gradient of protons across the membrane. We have developed a minimalist approach.[4] Thus in the same way that the architect may build a *maquette*, a three-dimensional small-scale model of a proposed building to evaluate the finished construction, a synthetic maquette of these complex biological systems can be conceived and developed as a means to comprehend the requirements for their function.

Robertson et al.[5] designed and successfully created a maquette of the *b*-cytochrome subunit of cytochrome bc_1. Figure 1 illustrates the principal synthetic steps involved. A 31-amino-acid peptide, α, was linked via a N-terminal cysteine disulfide bridge to form a helix-loop-helix, α_2, which spontaneously self-assembles in aqueous solution to form a dimer: $[\alpha_2]_2$. The dimer−monomer K_D value was less than 10^{-11} M as reported by Rabanal et al.[6] These synthetic four helix bundles possess a well-developed hydrophobic core[7] and are able to coordinate by bis-histidyl ligation Fe(III) protoporphyrin IX (heme) with a K_D ranging from 10^{-9} to 10^{-6} M.[5] The bundles have proven themselves to be viable molecular maquettes of hemoproteins and offer a novel way to study the structure and function of their more elaborate natural counterparts.

In this report, we investigate the adsorption of several hemoprotein maquettes on silanized quartz. Interest in the modification of solid surfaces by deposition of organic or biological molecules has gained increasing momentum the past decade,[8] drawn by the potential not only for applications in chemical[9] and biomedical sensing[10] but also in the analysis of the structure and the functionality of complex molecules. Typically, there are two different approaches to build ultrathin films on solid supports. Using the Langmuir−Blodgett (LB) balance, monolayers are assembled at the gas−water interface and then transferred onto a substrate. For self-assembly, synthetic or biological materials are initially dissolved in aqueous or organic solvent; immersion of a pretreated substrate in this solution is followed by chemical attachment of the solutes to the surface, leading to thermodynamically stable monolayers.

* Correspond with Denis Pilloud, B501 Richards Building, Johnson Research Foundation, Department of Biochemistry & Biophysics, School of Medicine, Philadelphia, PA 19104. Tel: (215) 898-5668. Fax: (215) 898-0465. E-mail: pilloud@mail.med.upenn.edu.

† Present address: Department of Chemistry, Rutgers University, Newark, NJ 07102.

S1089-5647(97)03348-8 CCC: $15.00
Published on Web 02/20/1998

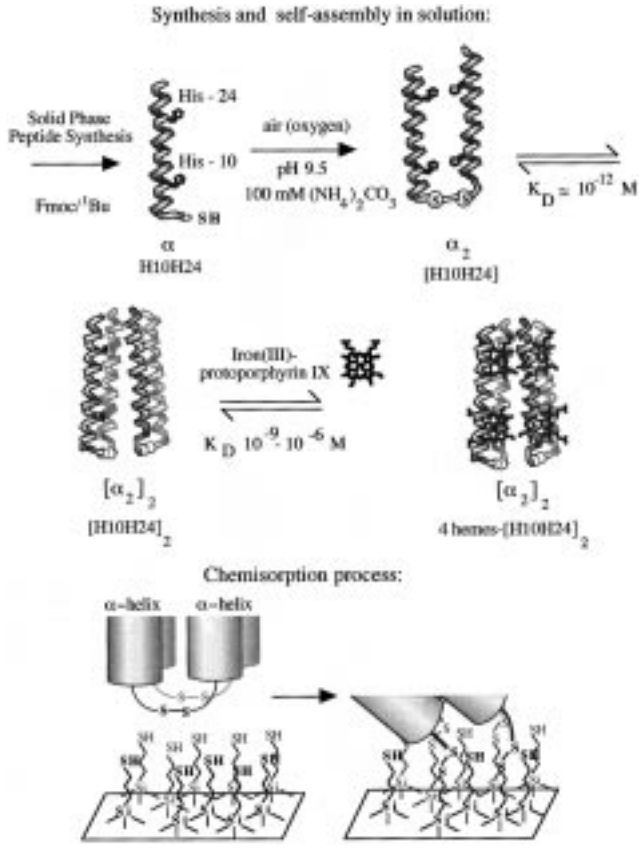

Figure 1. Solid-phase peptide synthesis produced the 31-amino-acid peptide, α, which is oxidized to form a di-α-helical unit, α_2, when exposed to oxygen at basic pH. Two α_2 units self-assemble into a four-α-helix bundle, $[\alpha_2]_2$, and coordinate hemes by bis-histidyl ligation. To fix the $[\alpha_2]_2$ onto a silanized quartz, the peptides were covalently attached to the substrate by exchange reaction between the disulfides bridges and the thiols of the silanized quartz. Throughout this work, the typical buffer solution contains 100 mM KCl and 50 mM TRIS, pH 8.2. For the formation of the SAMs, the concentration of $[\alpha_2]_2$ was 0.05 mM.

The two approaches are compared in Table 1; see also Netzer et al.[11]

The proteins selected for the investigations reported here were equipped with histidines positioned to bind iron protoporphyrin. The first two were described by Robertson et al.:[5] $[H10A24]_2$ ligates two and $[H10H24]_2$ ligates four hemes/bundle. The third protein, $[H10H24\text{-}L6I,L13F]_2$, a modification of these prototypes, shows as described a singular well-defined structure as demonstrated by NMR spectroscopy and has very similar heme affinities to its prototype $[H10H24]_2$.[12] The construction of films of these proteins is summarized at the bottom of Figure 1. The work presented compares two methods of assembly of the proteins on a silanized quartz surface. We investigate the orientation of the hemes and α-helices at the surface by UV/vis linear dichroism and circular dichroism (CD) spectroscopy. The absorption spectra in solution with the hemes oxidized, reduced and reduced with CO-bound are compared with the self-assembled monolayers (SAMs) and with the cytochrome c_3 described by O'Connor et al.[13]

Experimental Methods

Chemicals and Solvents. Tris[hydroxymethyl]aminomethane (TRIS), NaCl, and imidazole (fluorescence quality) were purchased from the Sigma Chemical Co. (St. Louis, MO). Pyridine, acetic anhydride, diethyl ether, trifluoroacetic acid, iron(III) protoporphyrin IX chloride, dimethyl sulfoxide (DMSO), and (3-mercaptopropyl)trimethoxysilane (MPS) were purchased from the Aldrich Chemical Co. (Milwaukee, WI). Ethanedithiol was obtained from Fluka (Ronkonkoma, NY) and 5,5′-dithiobis(2-nitrobenzoic acid) (DTNB) from Pierce (Rockford, IL). NovaSyn PR-500 resin and lauryldimethylamine oxide (LDAO) were purchased from Calbiochem-Novabiochem (La Jolla, CA). Fmoc-protected amino acid pentafluorophenyl esters were purchased from PerSeptive Biosystems (Framingham, MA) with the exception of Fmoc-L-Arg(Pmc)-OPfp which was obtained from Bachem (King of Prussia, PA). Sodium dithionite and 2-propanol (HPLC grade) were purchased from J. T. Baker (Phillipsburg, NJ), and NOCHROMIX salt was obtained from Godax Laboratories Inc. (New York, NY). Water was purified using a Milli-Q water system from the Millipore Corp. (Bedford, MA).

Peptide Synthesis. All peptides were synthesized by solid-phase methodology using the standard fluorenylmethoxycarbonyl/*tert*-butyl (Fmoc/^{t}Bu) chemistry as described previously.[5,12] Each peptide was purified and characterized by high performance liquid chromatography (HPLC) and mass spectrometric analysis. The peptide concentration in aqueous solution was determined by UV absorption of the tryptophan residue using[5] $\epsilon_{280} = 5{,}700\ \text{mol}^{-1}\ \text{cm}^{-1}\ \text{helix}^{-1}$. The amino acid sequence of the three different peptides studied are described in Table 2: (1) H10A24 has one alanine and one histidine at the 10 and 24 position, respectively, in each α-helical unit as described by Robertson et al.[5] After oxidation and self-assembly, it forms a four-helix bundle named $[H10A24]_2$ and 2 hemes-$[H10A24]_2$ after coordination to 2 porphyrins. (2) The bundle $[H10H24]_2$ ligates 4 hemes and was also characterized by Robertson et al.[5] (3) H10H24-L6I,L13F is a variant of the prototype H10H24, with the leucines at the 6 and 13 positions replaced by isoleucine and phenylalanine, respectively.[12]

Solution Molecular Weight Determination. The aggregation state of the proteins in aqueous solution was characterized by size exclusion chromatography as described previously.[5,6]

Preparation of the Solutions of Hemoproteins. The solutions of hemoproteins were prepared according to the procedure reported by Robertson et al.[5] An aqueous solution containing 0.02 mM 31-amino-acids peptides with unreacted cysteines was exposed to air to allow the cysteines to oxidize to form disulfide bonds and α_2 which, as shown in Figure 1, spontaneously dimerizes to $[\alpha_2]_2$. Heme was incorporated into $[\alpha_2]_2$ from a stock solution of 5 mM Fe(III) protoporphyrin IX in DMSO by successive additions of 0.1 heme per binding site until 0.99 heme/site was reached. During each addition, the solution was well stirred and then allowed to equilibrate for 5 min. The final concentration of DMSO in the aqueous solution was always lower than 1:200 (v:v). The heme incorporation was monitored by the increase of the Soret band[5] maximum, between 410 and 412 nm ($\epsilon = 100\,000\ \text{M}^{-1}\ \text{cm}^{-1}$). The solution of hemoproteins was finally concentrated from 0.02 to 0.2 mM by ultracentrifugation using Centricon-3 centrifugal concentrators obtained from Amicon, Inc. (Beverly, MA).

Absorption Properties of Heme Dissolved in LDAO. Aliquots of a stock solution of 0.1 mM heme in 10 mM LDAO were added to a 10 mM LDAO solution (Figure 2). Between each addition and after the solution was allowed to equilibrate for 5 min, the absorption spectrum was recorded.

Preparation of the Substrate. The quartz slides (10×25 mm^2) were purchased from Esco Products, Inc. (Oak Ridge, NJ). In certain situations, for instance, for circular dichroism and UV absorption spectroscopies of the SAMs, the exterior

TABLE 1: Comparison between Langmuir−Blodgett and Self-Assembling Techniques[a]

self-assembling	Langmuir−Blodgett
The adsorption is a spontaneous process, leading to thermodynamically equilibrated final films structures, depending essentially on the interactions between the components of the layer and between the film and the substrate.	The film compressed at the gas−water interface, can lose its structure upon or after the transfer to the substrate.
The adsorbate does not need to be water "compatible", i.e., inert toward water.	The adsorbate needs not only to be water compatible but to be also amphiphilic to form a stable monolayer at the gas−water interface.
The adsorbate is covalently linked to the substrate; therefore the film is less subject to desorption, and the diffusion of its components inside the layer is minimized.	To avoid changes in the structure of the film, often the sample has to be maintained constantly in aqueous solutions. Intralayer diffusion can cause structural modifications of the monolayer.
No special equipment is necessary.	To compress the monolayer and to transfer it to the substrate, a LB trough is necessary.
The structure of the adsorbate has to be characterized in solution and on film only.	The structure of the adsorbate has to be characterized not only in solution and on film but at the gas−water interface too.
The control of the orientation of the film at the surface (lying flat or standing perpendicular to the substrate) can eventually be achieved by the formation of mixed monolayers of the adsorbate with small polymers (e.g., polyphenyls) to give more rigidity to the film.	Compressing the film usually permits control of the orientation of the adsorbate at the surface, provided the sample conserves its integrity.

[a] Both methods have their advantages and disadvantages. indeed, a combination of techniques may provide the best film quality and structural control. For example, the substrate can be chemically modified by silanation before its dipping in the LB trough to modify the polarity of the surface or/and to attach covalently the adsorbates.

TABLE 2: Amino Acid Sequence of the Three Peptides Studied

1 10 24 31

H10A24:

Ac-CGGGE**L**WKL**H**EE**L**LKKFEELLKL**A**EERLKKL-*CONH*$_2$

H10H24:

Ac-CGGGE**L**WKL**H**EE**L**LKKFEELLKL**H**EERLKKL-*CONH*$_2$

H10H24-L6I,L13F:

Ac -CGGGE**I**WKL**H**EE**F**LKKFEELLKL**H**EERLKKL-*CONH*$_2$

and the interior of a 1 mm quartz cell were coated to provide four single monolayers. The quartz was then chemically cleaned by immersion in fresh NOCHROMIX acid[14] at room temperature for about 1 h, rinsed with H_2O, and then flushed with argon. The quartz was silanized by using the procedure described by Goss et al.[15] The MPS, used as received, was applied to the quartz slides from a boiling solution of 2-propanol. After a solution of 0.1 mL of MPS dissolved in 20 mL of 2-propanol was brought to reflux, the cleaned and dry substrates were immersed for 10 min and then carefully rinsed with the solvent, blown dry with a jet of argon, and cured in a drying oven at 100−107 °C for 10 min. The curing step is crucial to the performance of the coupling agent. After the completion of these steps, the slides appeared as clear and clean as before the MPS treatment.

Quantitative Determination of Free Thiols on the Substrate. Free thiols on the substrate were assayed using the Ellman's reaction[16] and measured spectroscopically as follows. The slide was completely immersed in a 1 mL solution of DTNB, pH 9 (Figure 2). The reaction was monitored at 410 nm. During the measurement, the sample remained in the cuvette, completely covered by the solution which was gently stirred. The reaction between the deprotonated DTNB and the thiol produces the 2-nitro-5-thiobenzoate anion (TNB) with a molar absorption coefficient (ϵ) of 14 150 M^{-1} cm^{-1} at 412 nm and a maximum at 409.5 nm (pH 7.3, 100 mM phosphate buffer).[16] The ϵ of TNB in 100 mM TRIS, pH 9, was determined by reacting DTNB with L-cysteine hydrochloride: 14 600 M^{-1} cm^{-1} at 410 nm.

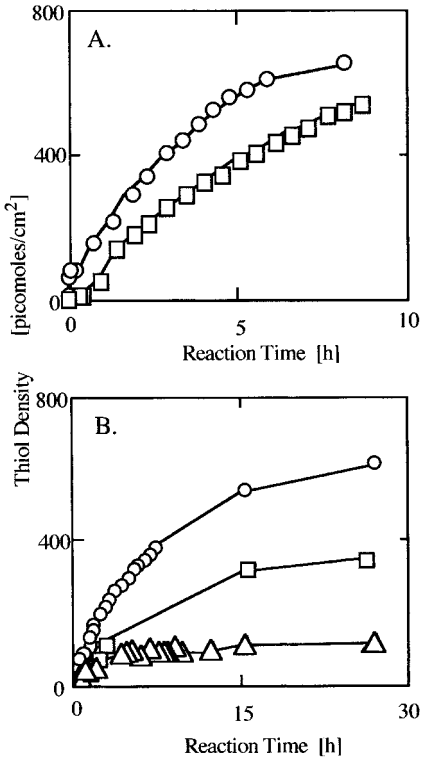

Figure 2. The density of thiols on MPS-treated quartz slides is represented versus the duration of the immersion of the slide in 1 mL of solution of 0.005 mM DTNB, 100 mM TRIS, pH 9, when (A) the coating was realized by one (circles) or by two (squares) silanation−curation processes and (B) after keeping the freshly coated slides overnight in argon (circles), exposed to air (squares), and to oxygen (triangles) prior to testing with the Ellman's reagent.

Formation and Chemical Treatment of SAMs of Synthetic Apo- and Hemoproteins onto the Substrate. A quartz cell

was placed into 0.2 mM apo-$[H10A24]_2$ solution for 8 h. After further immersion of the cell for 2 h in 1 M NaCl followed by washing with water and flushing with argon, hemes were incorporated by dipping the cuvette into a buffer solution of 0.025 mM heme at different time intervals (Figure 5). Between each immersion, the cell was washed with water and flushed with argon and its absorption was recorded. After more than 1 h of immersion, the absorption of the heme reached a plateau (Figure 5). There were two kinds of interactions of the porphyrins with the film: physisorption (van der Waals and electrostatic interactions) and chemisorption (bis-histidyl ligation). The physisorbed porphyrins were removed in the same way as for heme incorporation, but this time the sample was immersed in buffer containing first 2 M NaCl (Figure 6) and then 1 M imidazole (Figure 7).

The formation of SAMs from solutions of preformed hemoproteins was achieved by immersion of a quartz slide into a solution of 0.2 mM heme-$[H10H24]_2$ or heme-$[H10H24]_2$ or heme-$[H10H24\text{-}L6I,L13F]_2$ for 8 h. After washing with water, the films were kept in 1 M NaCl for 2 h to remove physisorbed hemoproteins.

Reduction and Interaction with Carbon Monoxide. A silanized quartz slide coated with synthetic hemoproteins was washed and placed into a 1 cm × 1 cm cuvette filled with 3 mL of buffer (Figure 11). After the cuvette was thoroughly degassed with argon for 30 min, 0.05 mL of buffer containing 0.5 mM sodium dithionite was added to reduce the hemes. The effect of carbon monoxide on the films of reduced hemoproteins was observed by bubbling pure CO for 5 min. During the whole experiment, the solution was maintained strictly anaerobic.

Circular Dichroism Spectropolarimetry. Quartz cells of 1 mm path length were placed in a circular dichroism spectropolarimeter Aviv 62DS, oriented perpendicularly to the beam. One quartz cell silanized with MPS only, was used as reference. A second silanized cuvette was immersed into a solution of 0.2 mM of apo-$[H10A24]_2$ overnight. After the cuvette was washed thoroughly with water followed by flushing with argon, the CD spectra were recorded and averaged 10 s every nanometer.

Absorption Spectroscopy and Linear Dichroism. Absorption spectra were recorded on a Perkin-Elmer UV/vis spectrophotometer Lambda 2. Measurements were performed with the slide immersed in buffer or in air. In the first case, a 1 × 1 cm^2 quartz cell cleaned by immersion for at least 1 h in NOCHROMIX acid was washed with water and, after drying, was finally filled with filtered buffer. The quartz coated with hemoprotein was then placed into the cuvette. A reference baseline was recorded with a cleaned quartz slide. At this point, it is important to notice that the quality of the spectra is extremely sensitive, especially in the UV region, to (1) the degree of cleanliness of the glassware used (it was cleaned as often as possible by immersion in fresh NOCHROMIX acid) and (2) the presence of particles in suspension in the buffer, which was always filtered twice using HPLC syringe filters with 0.2 μm pore size. For measurements performed in air, the samples were washed with water, flushed with argon, and then were positioned in the instrument using a homemade slide holder. For UV absorption, four slides instead of one were used to improve the quality of the spectra. For linear dichroism measurements, a UV dichroic polarizer from Oriel Corp. (Stratford, CT) sensitive from 230 to 770 nm was placed between the incident measuring beam and the sample. A baseline reference was recorded by using a quartz slide.

Results

Density of Thiols on Quartz Coated with MPS. The homogeneity of the thiolated surface of the silanized quartz is important in obtaining a complete uniform coverage of the hemoprotein maquettes. Goss et al.[15] silanized quartz with MPS for the fabrication of vapor-deposited gold electrodes. They observed a nonuniform adhesion of the gold to the surface when only one silanation−curation step was applied. In our work, we did not observe an improvement in the density of the thiols at the surface by additional treatment with MPS. On the contrary, when the silanation−curation was carried out one additional time, a decrease of the thiols density by 15% was observed (Figure 2A), probably due to the formation of disulfide bonds at the surface. Disulfide bonds can bind to gold[17] but are not reactive with Ellman's reagent.[16] After a single treatment with MPS and if we reasonably consider the reaction of the free thiols with DTBN as complete, the density observed after 6 h was 675 ± 50 pmol/cm^2 or 25 ± 2 $Å^2$ per thiol (Figure 2A). Considering the density of 20 $Å^2$ per silanol group for a fully hydrated surface of native oxide[18] and of 21 ± 3 $Å^2$ per alkylsiloxane group,[19] the surface appears to be almost totally covered. Therefore, SAMs were built onto quartz pretreated by only one silanation−curation step.

To establish how long the quartz slides can be stored after silanation before a degradation of the surface occurs, they were kept overnight under different environments. The thiols densities of the slides kept under argon atmosphere, avoiding any contact with oxygen, were very similar to those freshly silanized (Figure 2A,B). However, after overnight exposure to air, the thiols coverage decreased by 55%, and after exposure for the same time to pure oxygen there was an 82% decrease. In conclusion, silanized quartz slides with MPS can be stored for a short period of time under a controlled atmosphere, but in this work, they were always immersed in the protein solution within 30 min after the silanation.

UV Absorption of the Apoprotein. The UV absorption of a SAM of $[H10A24]_2$ on a quartz cuvette is shown in Figure 3A. The measurements were performed with the films exposed to air, out of solution. If the tryptophan ϵ value of 5700 M^{-1} cm^{-1} at 280 nm remains unchanged in the film, the density of one single α-helix can be estimated to 110 ± 30 pmol/cm^2 or 150 ± 40 $Å^2$/helix. The spectra of SAMs of apo-$[H10H24]_2$ are shown in Figure 3B. In these measurements, the slides were kept in solution at all time. The figure shows the UV absorption of one single slide (two monolayers) and of the four slides in series together (total of eight SAMs). The absorption of a solution of apo-$[H10H24]_2$ (dashed) is also presented for comparison. The density of α-helices was determined using the spectra of the four slides: 100 ± 20 pmol/cm^2 or 170 ± 30 $Å^2$/helix. This value is close to the density observed for the dry films, within the experimental error. Figure 3 shows that monolayers maintained in solution display better quality UV absorption than dry films. When the slides are exposed to air, the surface becomes contaminated and the quality of the spectra decreases rapidly with time. In solution, this observation is still true, but if the film is manipulated with care, the degradation can be minimized.

Circular Dichroism. Circular dichroism measurements of SAMs of apo-$[H10A24]_2$ demonstrated the conservation of the α-helicity of the peptides upon adsorption. The spectra also provides some information about the orientation of the helices at the surface. Figure 4 shows that differences are clearly visible between CD of solution and of film. They can be explained by (1) a partial loss of helicity, (2) the presence in the film of

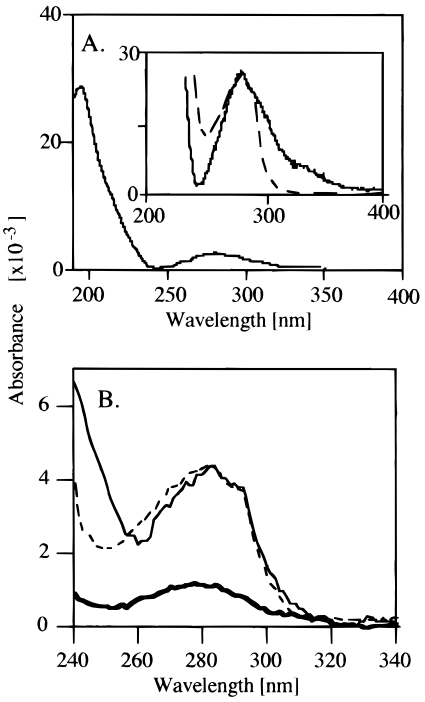

Figure 3. (A) UV spectroscopy of four single monolayers of apo-$[H10A24]_2$ on silanized quartz and exposed to air. The inset shows the summation of 10 spectra (solid) compared to the normalized absorption in solution (dashed). (B) The absorption of one single quartz slide coated with apo-[H10H24] (solid thick line) immersed in buffer and the spectrum of 4 slides placed together in the same cell (solid thin line) filled with buffer are compared to the spectrum of apo-$[H10H24]_2$ in solution (dashed line). The experimental conditions are the same as in Figure 1.

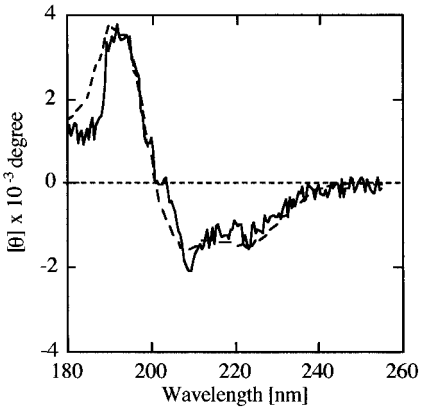

Figure 4. The CD spectrum of four SAMs of apo-$[H10A24]_2$ (solid) onto a quartz cuvette is compared to the CD in solution (dashed) normalized with the band at 193 nm of the film. The experimental conditions are the same as in Figure 1.

single-stranded α-helices without a coiled coil structure, and (3) the orientation of the peptides at the surface. These three possibilities will be discussed later.

Incorporation of Heme in a SAM of Apo-$[H10A24]_2$. Heme adsorption in a monolayer of apo-$[H10A24]_2$ occurs in minutes time scale. After 30 min, the absorption reaches 95% of the value observed after 4 h exposure to the heme solution (Figure 5). But judging from the intensity and the position of the Soret band, the porphyrins adsorbed are not all bis-histidyl ligated. A film containing only bis-histidine coordinated iron-(III) porphyrins is expected to show a distinct Soret band at 410 nm with an intensity of 0.0055 A/monolayer (estimated from the density found by UV spectroscopy: 110 pmol of

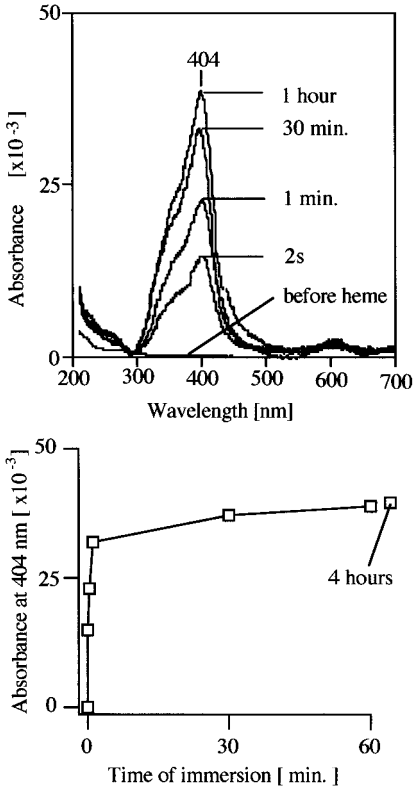

Figure 5. Absorption of four single monolayers of H10A24 after immersion in a buffer solution of 0.025 mM of heme during 0 s, 2 s, 1 min, 30 min, and 1 h. No significant change was observed after 1 h. The experimental conditions are the same as in Figure 1.

α-helices/cm^2 or 150 Å^2/α-helix and using $\epsilon = 100\,000$ M^{-1} cm^{-1}), instead of the observed absorption of 0.0082 A/monolayer at 404 nm. Another indication of the existence of free porphyrins in the SAM is the presence in the spectra of a small absorption band located at 610 nm (Figure 5), typical of free hemes.[20]

Removal of Physisorbed Hemes with NaCl. To differentiate between the different types of physisorbed porphyrins, they were desorbed from the film one species at the time. The first step involved the immersion of the cuvette in 2 M NaCl (Figure 6). This treatment led to a decrease in the absorption of the film (Figure 6A). The difference spectrum between the unwashed minus NaCl-washed film (i.e., the spectrum of the physisorbed porphyrins) presented in Figure 6B (solid line) is very similar to the absorption of hemes in micelles of LDAO at micromolar concentrations (dashed line). Thus it can be suggested that the physisorbed porphyrins in the film are located in a nonpolar environment and perhaps in close contact with each other. As indicated in Figure 6D, when hemes are added in LDAO solution at concentrations lower than 0.01 mM, the Soret band at 402 nm increases linearly with the concentration, giving ϵ_{402} of 109 000 M^{-1} cm^{-1}. At concentrations higher than 0.01 mM, the Soret band broadens and shifts to 399 nm but still depends linearly on the concentration of the heme, with a slope decrease close to 50% ($\epsilon_{402} = 58\,000$ M^{-1} cm^{-1}), apparently due to dimerization of hemes in the micelles. The density of the hemes removed by NaCl from the film of heme-$[H10A24]_2$ was estimated to 52 pmol/cm^2 (320 Å^2/heme), considering $\epsilon_{402} = 58\,000$ M^{-1} cm^{-1}.

Desorption of Physisorbed Hemes with Imidazole. Immersion of the SAM of heme-$[H10A24]_2$ in a solution of imidazole for 30 min removed more porphyrins from the film. Figure 7A shows the residual absorption was typical of bis-

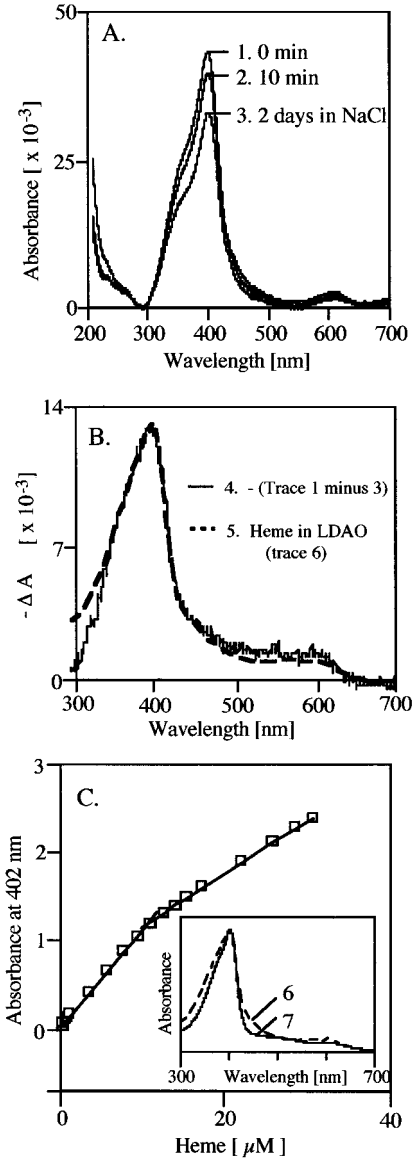

Figure 6. Removal of the physisorbed hemes from the film with NaCl and comparison of its absorption with the spectra of hemes in micelles of LDAO. (A) After incorporation of the heme in the film, the sample was immersed in a solution of 2 M NaCl and 50 mM TRIS, pH 8.2, for 0 s, 10 min, and 2 days. (B) The difference between the absorption before treatment and after 2 days (trace 4, solid) is compared to the normalized spectra of 0.019 mM heme in LDAO (trace 5, dashed). (C) Absorbance at 402 nm versus the concentration of heme in a solution of 100 mM KCl, 10 mM potassium phosphate, pH 8, and 10 mM LDAO. In the inset, the normalized spectra of 0.8 μM (trace 6, solid) and of 17 μM (trace 7, dotted) of heme in LDAO are compared.

histidyl hemes with a pronounced Soret band at 410 nm. Figure 7B shows that porphyrins desorbed by imidazole and aqueous hemes have very similar absorption spectra. With an absorbance of 0.0027 A per monolayer at 390 nm and $\epsilon_{393} = 55\,600$ M^{-1} cm^{-1} reported by Silver et al.[20] for iron(III) protoporphyrins IX in solution, the density of these hemes is estimated to 49 pmol/cm^2, close to the density of the first type removed by NaCl. Finally, the remaining spectra, with an absorbance at 410 nm of 0.0055 A per monolayer and considering $\epsilon_{410} = 100\,000$ M^{-1} cm^{-1} reported by Robertson et al.,[5] the density of the ligated hemes is evaluated to 55 pmol/cm^2 (300 Å^2/heme).

Reversibility of the Adsorption/Desorption Process. The process consisting in adding hemes to SAMs of apoproteins followed by removing the physisorbed porphyrins was completely reversible. After the treatment with imidazole, when films of heme-[H10A24]$_2$ were exposed again to a heme solution, their absorption spectra were similar to the spectra reported in Figure 5, when the SAMs of apo-[H10A24]$_2$ were first immersed in the heme solution. Moreover, when the cuvette was again immersed in a solution of imidazole for 1 h, a similar spectrum as described in Figure 7A was obtained with a Soret band at 410.5 nm and an intensity of 0.0055 A per monolayer (not shown).

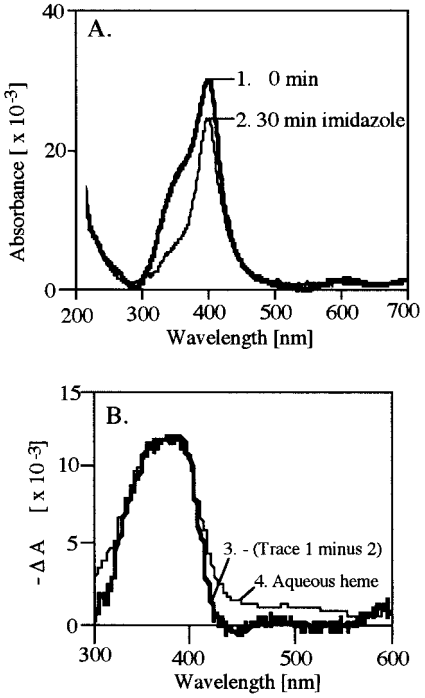

Figure 7. Removal of physisorbed hemes with imidazole. (A) Absorption of four single monolayers of H10A24 after immersion for 2 days in 2 M NaCl (trace 1, thick) and 30 min in 1 M imidazole (trace 2, thin). (B) The difference between these two spectra (trace 3, thick) is compared with the absorption of heme in buffer (trace 4, thin). The buffer is the same as described in Figure 6. The pH of the imidazole solution was adjusted to 8.2 by adding 1 M HCl solution.

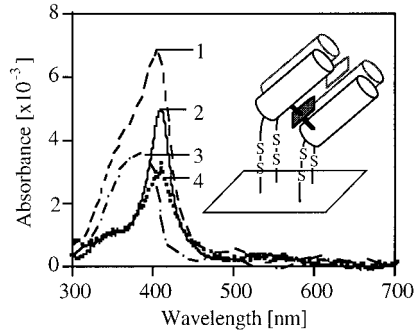

Figure 8. The absorption of silanized quartz after coating with 2 hemes-[H10A24] (1) decreased after immersion of the slide for 5 h in imidazole solution (4). The trace (1) is treated as a linear combination of the spectrum of unligated hemes (3) and of the coordinated porphyrins (2). During the measurements, the sample was immersed in buffer. All conditions are the same as in Figure 1.

Formation of SAMs from a Solution of Preassembled Synthetic Hemoproteins. The adsorption of [H10A24]$_2$ ligating 2 hemes leads to the formation of a SAM with only one coordinated heme/bundle. The result is shown in Figure 8. After coating, the spectrum with a broad Soret band at 404 nm indicates that upon adsorption a significant fraction of the hemes lost their bis-histidyl ligation (dashed, trace 1). To reveal the

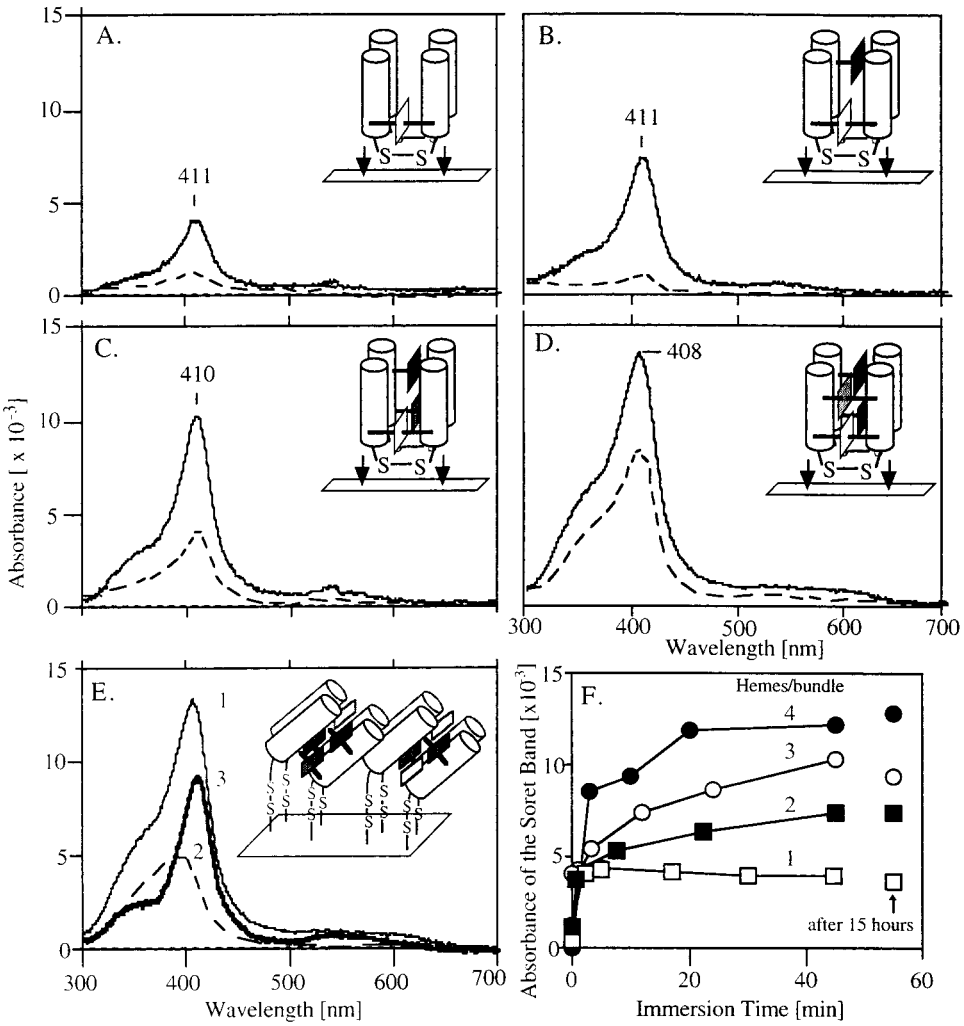

Figure 9. From A to D, absorption of a silanized quartz slide after dipping for a few seconds (dashed) and for 1 h (solid) in buffer containing 1 (A) heme-, 2 (B) hemes-, 3 (C) hemes-, and 4 (D) hemes-[H10H24-L6I,L13F]$_2$. Analysis of the spectra C and D revealed the presence of unligated porphyrins in the film, as shown in E. Subtracting the absorption of uncoordinated hemes (trace 2, dashed), obtained after addition of the spectra of porphyrins desorbed with NaCl and imidazole (from Figure 6B and 7B), from the absorption of SAMs of 4 hemes-[H10H24-L6I,L13F]$_2$ (trace 1, thin) revealed the absorption of the still bis-ligated porphyrins (trace 3, thick). The same procedure was repeated for SAMs of 3 hemes-[H10H24-L6I,L13F]$_2$. The inset of the Figure 9E shows a schematic drawing illustrating an idealized SAM composed of an equal population of synthetic protein with 2 and 3 ligated hemes/bundle, tilted at 40° relative to the substrate. In F, the increase of the Soret band is shown at different times of immersion. All conditions are the same as in Figure 1.

hemes remaining coordinated, the absorption of the unligated hemes had to be established first. This was estimated by combining the spectrum of the porphyrins removed with NaCl (trace 4 in Figure 6B) and imidazole (trace 3 in Figure 7B) from the SAM of heme-[H10A24]$_2$. The total film spectrum was then modeled as a linear combination of this unligated heme spectrum and the residual bis-histidyl ligated SAM spectrum after extensive desorption with NaCl and imidazole (Figure 7A, trace 2). The absorbance of the porphyrins remaining bis-histidyl coordinated upon adsorption was estimated to 0.0025 A/monolayer (Figure 8, trace 2). This corresponds to a density of 25 pmol/cm^2, approximately half the value observed with the apoprotein (55 pmol/cm^2). Thus, it appears that the formation of a SAM from 2 hemes-[H10A24]$_2$ yields only one bis-histidyl heme/bundle. Immersion of the film in 1 M imidazole for 3 h was necessary to remove the unbound porphyrins, but most probably some ligated porphyrins were also desorbed from the film as well, since the signal observed (dotted, trace 4) is only 65% of the expected absorption for 1 heme/bundle (trace 2).

In contrast to films of heme-[H10A24]$_2$, monolayers of heme-[H10H24]$_2$ constructed from a solution of [H10H24]$_2$ with 2, 3, and 4 ligated hemes/bundle retained the coordination of 2 hemes. The absorption spectra of a slide after exposure to a solution of 2 hemes-[H10H24]$_2$ is typical of bis-histidyl hemes with the Soret band at 412 nm and identical to solution;[5] even the α- and β-bands are visible (Figure 11). The intensity of the Soret band of 0.004 A per monolayer is 65% of the signal observed for SAMs of apo-[H10A24]$_2$ after adding heme and after treatment with imidazole (Figure 7). When monolayers are formed from solutions of [H10H24]$_2$ binding 3 and 4 hemes/bundle, only two hemes retain their ligation to the histidines after formation of the SAM. However the others remain associated with the film displaying the characteristic absorption of hemes in an apolar environment (such as in Figure 6B).

Parallel studies were conducted on heme-[H10H24-L6I,-L13F]$_2$, the singular structured variant of the prototypes. The results are described in Figure 9. Like heme-[H10H24]$_2$, 2 hemes/bundle conserve their ligation upon SAM formation. Figure 9A,B shows that when the slides are coated with heme-[H10H24-L6I,L13F]$_2$ preformed with 1 and 2 hemes/bundle, the spectra are typical of bis-histidyl hemes with an absorbance at 412 nm of 0.002 and 0.004 A/monolayer, respectively. Assuming the same ratio heme/α-helix as in solution, the density

of the α-helices can be estimated to 90 ± 20 pmol/cm^2 or 190 ± 30 Å^2/helix. When 3 and 4 hemes were incorporated in the $[\alpha_2]_2$ in solution, the presence of non bis-histidyl ligated porphyrins in the film is revealed by the hypsochromic shift of the Soret band (from 411 nm in Figure 9A,B to 408 nm in Figure 9D). However, [H10H24-L6I,L13F]$_2$ conserves upon adsorption more than the 2 ligated hemes/bundle observed with [H10H24]$_2$. The monolayer probably consists of an equal population of $[\alpha_2]_2$ binding 2 and 3 hemes, as described in Figure 9E. This model was deduced using the following procedure. Both bis-histidyl ligated and uncoordinated hemes contribute to the spectra of 3 and 4 hemes [H10H24-L6I,L13F]$_2$ in Figures 9C,D. To distinguish between these two contributions, the absorption of the unligated hemes had to be established first. It was estimated in the same way as described above for 2 hemes-[H10A24]$_2$. A similar linear combination of unligated and ligated heme spectra was used to analyze the total SAM spectrum (Figure 9). The absorption of unligated hemes was found 3 times lower in films of 3 hemes-[H10H24-L6I,L13F]$_2$ than in SAMs of 4 hemes-[H10H24-L6I,L13F]$_2$. In both cases, the spectra of bis-histidyl ligated hemes were identical. However, the ratio A(3 or 4 hemes-[H10H24-L6I,L13F]$_2$): A(2 hemes-[H10H24-L6I,L13F]$_2$) was 5:4, indicating that more than 2 hemes/bundle were ligated. To explain the distribution of the hemes in the film, we propose the following model: monolayers of 2 hemes-[H10H24-L6I,-L13F]$_2$ coordinates 2 hemes and no unligated hemes are present in the film. In SAMs of 3 hemes-[H10H24-L6I,L13F]$_2$, there is a distribution of hemoproteins with 2 bis-histidyl ligated and 1 unligated hemes as well as bundles with 3 bis-histidyl ligated and no unligated hemes. Similarly, the SAMs of 4 hemes-[H10H24-L6I,L13F]$_2$, as illustrated in Figure 9E, are constituted of a mixed population of hemoproteins with 2 bis-histidyl ligated and 2 unligated hemes and hemoproteins with 3 bis-histidyl ligated and 1 unligated hemes. This model satisfies the following observations: the same density for the bis-histidyl ligated hemes as well as the ratio 3:1 of uncoordinated hemes in 4 versus 3 hemes-[H10H24-L6I,L13F]$_2$ and the ratio of 5:4 for the ligated hemes in 3 and 4 versus 2 hemes-[H10H24-L6I,-L13F]$_2$. In Figure 9E, the absorption of SAMs of 4 hemes-[H10H24-L6I,L13F]$_2$ (trace 1) is described as a linear combination of the absorption of bis-histidyl hemes (trace 3) with the unligated porphyrins (trace 2). Figure 9F describes the kinetics of the adsorption of heme-[H10H24-L6I,L13F]$_2$. As in case of the incorporation of heme in SAMs of apo-[H10A24]$_2$ (Figure 5), the adsorption of the hemoproteins occurs in a time scale of minutes.

Linear Dichroism of the SAMs of Synthetic Hemoproteins. Linear dichroism of the hemes attached to the peptides can reveal their orientation on the surface of the quartz. When the orientation of the plane of polarization of the light was changed from horizontal (out of the substrate plane) to vertical (in plane), the absorption of the SAM decreased. This observation was quantified using eq 1 described by Blasie et al.,[21] which provides

$$D(\lambda) = \frac{A_h(\lambda)}{A_v(\lambda)}\left(2\sin^2\alpha_i\left[\frac{\sin^2\gamma^o_{av}}{2-\sin^2\gamma^o_{av}}\right]+\cos^2\alpha_i\right) \quad (1)$$

an estimate of the tilt angle of the porphyrin macrocycle plane relative to the substrate. In the equation, D is the dichroic ratio between the absorption of horizontally (out of plane) (A_h) to vertically (in plane) (A_v) polarized light. The incident angle, α_i, is the angle between the incident beam and the normal to the monolayer plane, and γ^o_{av} is the angle between the normal to the heme macrocycle plane and the normal to the monolayer plane. This relation between D and α_i includes two important assumptions: (1) The oriented monolayers possess a cylindrical symmetry about the normal to the substrate. In other words, there is an isotropic distribution of the hemes in the plane of the substrate but an anisotropic distribution of the hemes in the plane normal to the substrate. (2) The two transition moments of the hemes are $x-y$ polarized, i.e., they lie in the porphyrin plane at right angles to one another and they have equal probabilities.

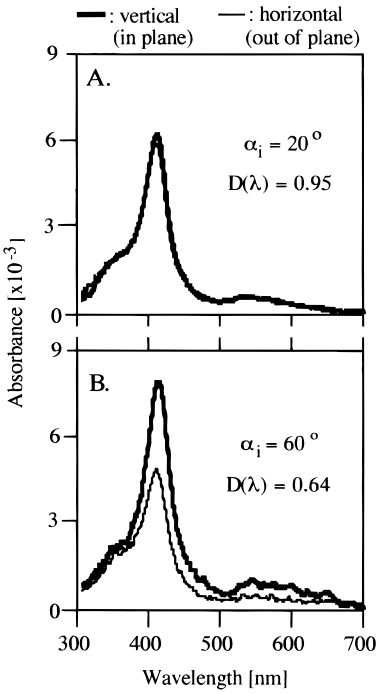

Figure 10. Linear dichroism of SAMs of 2 hemes-[H10H24]$_2$ on quartz silanized with MPS. Absorption spectra at two different positions of the sample relative to the incident beam with the light polarized vertically (thick) and horizontally (thin).

Monolayers of synthetic hemoproteins show a linear dichroism as illustrated in Figures 10C,D. Independently of the nature of the hemoprotein or of the process of fabrication of the monolayer, we found the average tilt angle γ^o_{av} to be 40 ± 2°. Therefore, if we consider the molecular plane of the porphyrins approximately parallel to the axis of the α-helices (±10°), the long axis of the assembly would lie at an angle around 40° relative to the surface. The insets in the Figures 9E and 12 illustrate idealized SAMs of hemoproteins, all of them oriented at 40° relative to the substrate. However, some distribution in the orientation of the hemoproteins at the surface is likely, with nonetheless a majority of them tilted at angle lying between 20° and 45°. The variation of γ^o_{av} of only 5° when α_i was changed from 20° to 75° suggests a good homogeneity of the film (Table 3).

Reduction and Interaction with Carbon Monoxide. Figure 11A describes the absorption of a 0.015 mM solution of 2 hemes-[H10H24]$_2$, in oxidized, reduced, and CO-bound reduced forms, and Figure 11B represents the absorption of the SAM. After the solution was degased and sodium dithionite was added, the spectra observed in solution and in film were almost identical, with the α-band at 558 nm clearly visible (Table 4).

The Soret band of the CO-treated hemes is located at 421 nm for both SAM and solution, but the α-band shows an hypsochromic shift by 4 nm in the film (Table 4). By correlation with the observations reported for cytochrome c_3[13] and since no residual spectra of ferrous bis-histidyl heme was

TABLE 3: Tilt Angle of the Plane of the Heme (γ^{o}_{av}) in SAMs of Hemoproteins Calculated for Different Incident Angles (α_i)[a]

α_i (°)	$D(\lambda)$	γ^{o}_{av} (deg)	$\pm\gamma^{o}_{av}$ (deg)
0	1.00	-	-
20	0.95	42	12
30	0.90	43	7
40	0.83	42	3
45	0.79	42	3
50	0.73	41	2
60	0.64	40	2
70	0.55	39	2
75	0.53	39	2

[a] The standard error on γ^{o}_{av} was determined using an error of 0.001 on the absorption and of 1° on α_i.

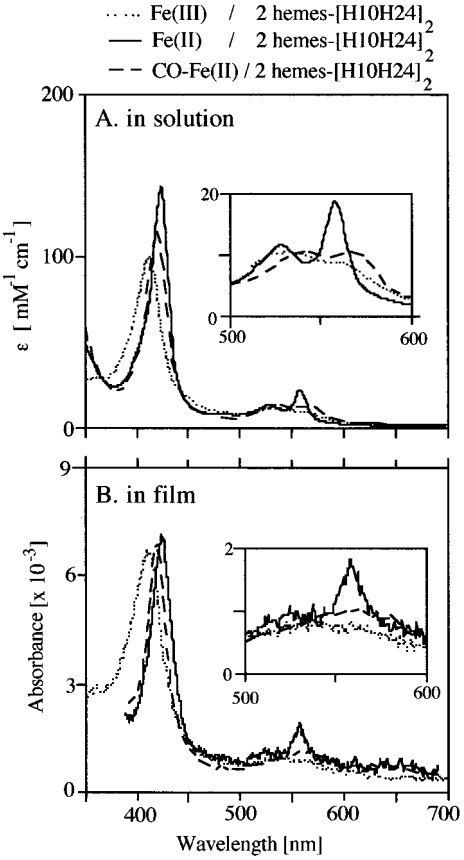

Figure 11. Absorption of 2 hemes-$[H10H24]_2$ in its oxidized (dotted), reduced (solid), and reduced/CO (dashed)-bound-forms: (A) solution of 0.015 mM of 2 hemes-$[H10H24]_2$ in buffer and (B) on quartz/MPS, with the slide immersed in buffer. The spectra were recorded every 0.5 nm, with a smoothing factor of 2 nm, but no averaging. The positions of the Soret, the α-, and β-bands are reported in Table 4. All conditions are the same as in Figure 1.

detected, the two porphyrins ligated to the peptide are interacting with CO by displacing one of the histidines. After the slide was washed with buffer, the absorption spectra of the oxidized hemes is observed, similar to the one shown in Figure 11B (dotted line) but with a loss of 30% of intensity. The desorption of hemoproteins weakly bound to the surface and/or the removal of the hemes from the film (the protoporphyrins are not covalently attached to the peptide) can be the cause of this decrease. Carbon monoxide does not appear to be responsible for this desorption, even if it has to displace one histidine to bind to the porphyrin. On the contrary, it seems to enhance ligation: after 1 h of degassing the solution with argon, the spectra of the film did not change, and even after immersing

TABLE 4: Absorption of Solution and Film of 2 Hemes-$[H10H24]_2$, Oxidized, Reduced, and CO Bound/Reduced[a]

band	α (nm)	β (nm)	Soret (nm)
	2 Hemes-$[H10H24]_2$		
solution			
Fe(III)	559	532	412
Fe(II)	558	528	424
Fe(II)−CO	568	540	421
SAM			
Fe(III)	558	534	411
Fe(II)	558	527	424
Fe(II)−CO	564		421
	Cytochrome c_3		
solution			
Fe(III)	530		410
Fe(II)	552	525	419
Fe(II)−CO	561	539	415

[a] For comparison, the absorption maxima of solution of cytochrome c_3 are also listed.[13]

the SAM in fresh buffer, still 10% of the hemes were ligated to CO. It seems probable that the desorption of hemes from the film occurs during the reduction: In solution of 2 hemes-$[H10H24]_2$, the intensity of the Soret band increased by a factor 1.5 (Figure 10A) after reduction, but in films, the increase was only by 1.2 (Figure 10B). Thus sodium dithionite added to the solution as reductant is probably responsible for the partial desorption of hemes from the film. Finally, monolayers of oxidized hemoproteins did not show any interaction with CO, no spectral change having being observed.

Discussion

The UV absorption of the tryptophans gives the first indication of the presence of peptides on the substrate (Figure 3). With a density evaluated between 130 and 190 Å^2/peptide, the peptides are probably not standing perpendicularly to the surface. Considering the area of 100 Å^2 (10 × 10 Å^2) one α-helix occupies on the surface when oriented perpendicularly to the substrate, and the area along the helix axis of 500 Å^2 (10 × 50 Å), the film is composed possibly by a close-packed monolayer of peptides lying at an angle estimated between 20° and 45°.

Circular dichroism shows that the peptides retain some helicicity upon adsorption. The fitting of the CD spectrum of $[H10A24]_2$ in solution with the CD spectra of α-helix and of unordered polypeptides described by Brahms et al.[22] gave a percentage of α-helicity of 84%, in agreement with the previously reported values.[5] However, it was not possible to estimate the α-helicity of the peptides in the SAMs. In fact, other factors influence the shape of the CD spectrum of peptides immobilized onto a substrate: The observed changes of the bands at 193, 208, and 224 nm (Figure 4) may be the result of tertiary structure alterations. In this regard, the ratio $[\theta]_{224}/[\theta]_{208}$ of 1.04 observed for $[H10A24]_2$ in solution is attributed to a coiled coil,[23] while a ratio of 0.78 in monolayers can be assigned to single-stranded α-helices.[23a] The orientation of the peptides on the substrate is certainly affecting the circular dichroism. As shown in studies of polypeptides oriented by electric field,[24e,f] by immobilization in lipid bilayer,[24a−d] and in LB films,[24g,h] the bands at 208 nm and at 224 nm are very sensitive to the α-helical axis orientation relative to the measuring beam. For example, de Jongh et al.[24b,c] analyzed the CD of oriented films of lipid−protein complexes. When the α-helices were adsorbed parallel to the surface of the substrate, a change in the CD similar to the one reported in Figure 4 was observed, in that the absolute

intensity at 208 nm was increased and the band at 224 nm was slightly decreased. By analogy and if we consider that the differences observed are due essentially to the orientation of the peptides on the quartz, the inclination of the α-helices of the hemoprotein maquettes relative to the surface is less than 45°. Two additional observations corroborate this last point: LB films of synthetic apopeptides on quartz pretreated with octadecyltrichlorosilane exhibited a circular dichroism not only similar to the SAMs but almost identical to the CD observed by de Jongh et al.[24b,c] for polypeptides oriented parallel to the surface.[25] On the other hand, the linear dichroism of the SAMs of heme-containing synthetic proteins, giving a tilt angle of 40° of the plane of the porphyrins relative to the surface of the quartz, strongly suggests a tilted orientation with, however, two important restrictions: (1) It is assumed that the plane of the hemes and the axis of the peptides are parallel, and (2) the value of 40° has to be taken with precaution. It means only that in average the hemes are tilted at 40°, and most probably a distribution of γ_{av}^{o} exists. Recently, Edminston et al.[26] and Wood et al.[27] determined the molecular orientation distribution of yeast cytochrome *c* onto SAM-coated glass, combining absorption linear dichroism and fluorescence anisotropy. They observed very different dispersions depending on the nature of the substrate: from ±20° to ±30° for thiol SAM-coated glass and ±6° for arachidic acid LB film. This difference is explained by multiple adsorptive interactions (electrostatic, van der Waals, covalent) between the protein and the thiol SAM-coated substrate and by almost exclusively electrostatic adsorption in the case of the LB film. In this particular case, the different modes of attachment of the cytochrome *c* to the thiol SAM-coated glass can be explained, at least partially by the low accessibility of the thiol tail groups on the SAM by the Cys102 of the cytochrome.[27] With the linear dichroism technique we used in this study, it is not possible to determine the amplitude of this distribution, but nonetheless, this method is attractive for prospective work in the study of new or modified films: This technique is very convenient to check the effect of the nature of the substrate, the peptides, or of mixed monolayers on the orientation of the hemes in the film. For example, SAMs with the hemes lying perpendicularly to the substrate will show a reverse linear dichroism relative to the one reported in Figure 10, with the vertically polarized more intense than the horizontally polarized absorption.

To be considered as an effective maquette of the cytochrome bc_1 complex, the synthetic peptides adsorbed on a surface must conserve their binding properties toward the heme. Not only coordinated but also unligated hemes were detected in films of apo-$[H10A24]_2$ after exposure to heme solution. By treatment with NaCl, followed by imidazole, we were able to distinguish between three species. Figure 12 describes the possible locations of these porphyrins. First, the less strongly adsorbed, removed with NaCl, can be located inside the hydrophobic core of the peptide, between the ligated hemes, because of their slow desorption from the monolayer (2 days in 2 M NaCl) and of their absorption very similar to the heme dissolved in micelles of LDAO. On the other hand, the spectra can be interpreted as a film of hemes adsorbed at the surface of the SAM. Excitonic interaction between proximal hemes can explain the bathochromic shift of the spectra and strong van der Waals interactions between the porphyrins and the surface of the film, the slow desorption. The second type, removed with imidazole, shows a similar absorption spectrum as that of hemes in water and is not desorbed by NaCl. It is possibly localized inside the film, in contact with each other and with the polar residues of the

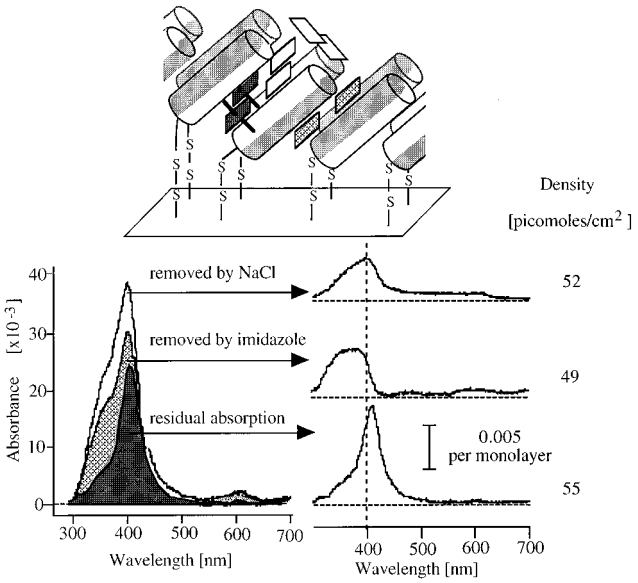

Figure 12. Schematic illustration of heme distribution in a monolayer of $[H10A24]_2$ after immersion in a solution of heme: The physisorbed hemes removed with NaCl (in white) can be located inside the hydrophobic interior of the peptide, or eventually at the surface of the film. The porphyrins desorbed with imidazole (patterned area) can occupy the space between the peptides, outside the hydrophobic core, in a polar environment. The hydrophilic part of the α-helices are represented in the gray area. Finally, the residual spectra, typical of bis-histidyl hemes, are assigned to the ligated porphyrins (in dark). In the cartoon, the idealized SAM is represented with the α-helices (cylinders) tilted at 40° relative to the surface.

peptide. Finally, the remaining porphyrins resistant to desorption are most certainly coordinated to the two histidines at the 10 positions. The presence of imidazole-ligated hemes in the film can be rejected: The difference spectra in Figures 6B and 7B show in both cases the desorption of hemes absorbing at wavelengths always lower than 405 nm. But no increase of the absorption was observed at higher wavelength, indicating that if imidazole ligates to uncoordinated hemes, the complexes do not stay in the film but are desorbed in the solution. The competition between imidazole and the histidines for the coordination to the hemes cannot be entirely excluded, leading to the formation in the film of porphyrins ligated to histidine and imidazole. But as the spectra of residual hemes is so similar to the absorption of the hemoprotein in solution, the possibility is unlikely. Finally, the similar density between the three types of hemes, 50−55 pmol/cm^2, and the total reversibility of the adsorption−desorption process suggest the occupancy of specific sites inside or at the surface of the film.

When complete synthetic hemoproteins were adsorbed onto silanized quartz, they were still able to conserve partially the coordination with the iron(III) porphyrins. Two kinetics in the time course of the adsorption can be sorted out. The initial sharp increase of the adsorption (Figure 9F) during the first minutes of immersion can be rationalized by rapid adsorption of an imperfect monolayer, probably driven by van der Waals interactions between the apolar residues of the interior of the peptide (from Leu or Trp) and the surface, and by exchange reaction between the cystines of the peptide and the thiols at the surface. Then a slower process follows, which can take minutes to hours. It consists of additional adsorption and consolidation, possibly involving the rearrangement of the bundles at the surface (e.g., formation of new hydrogen bonds and electrostatic interactions between the polar amino acids located at the exterior of the assembly, such as Glu or Lys).

This consolidation mechanism would not only improve the packing at the surface (for example, by increasing the tilt angle) but would create more room for the adsorption of additional hemoproteins. On the other hand, bis-histidyl ligated porphyrins in films formed directly from heme-$[H10H24]_2$ and heme-$[H10H24\text{-}L6I,L13F]_2$ were 88% less dense than in films constructed from apoproteins. A different structure between these two films can explain this lower coverage: The hemes by ligating the histidines rigidify the $[\alpha_2]_2$ in solution which therefore have more difficulty in modifying their configuration to form close-packed monolayers.

Finally, films of hemoprotein maquettes after reduction, were able to ligate CO. The CO complexes show interesting absorptions: The position of the Soret band at 421 nm is the same in film and in solution, but an hypsochromic shift of the α-band by 4 nm was observed (Table 4). Changes in the planarity of the iron and in the charge-transfer transition between the iron and CO, for example, electrostatic interactions between the peptide polar groups, especially the glutamates (Glu) and CO, can explain this observation.[2] Indeed an electrostatic effect of glutamate on heme redox potential has been observed in solution of these maquettes.[29] In human myoglobin, a similar observation was reported by Decatur et al.[30] The amino acid at position 68, because of its proximity to the heme pocket can have specific interactions with the ligand of the porphyrin, for example, with CO. In the native form, valine occupies this position and, because of its apolar character, does not interact with CO. The replacement of Val68 by Glu or Asp induced an hypsochromic shift of the α-band by 2 and 4 nm, respectively.

The hemoprotein maquette 4 hemes-$[H10H24]_2$ shows many similarities with the cytochrome c_3. In this natural protein, 4 hemes are covalently bound by thioether linkages to a single polypeptide consisting of 100−120 amino acids with a molecular weight of 13−15 kDA ($[H10H24]_2$ is composed of 124 amino acids with a molecular weight of 14−15 kDA). As in the hemoprotein maquette, 4 heme groups have histidines as axial ligands in both the fifth and the sixth coordination sites. The cytochrome c_3, when fully reduced, is able to ligate CO at the sixth coordination position of each of the 4 hemes. The cytochrome c_3 and 4 hemes-$[H10H24]_2$ both show low redox potentials (from −240 to −357 mV[13] and from −150 to −250 mV[5] for the natural and the synthetic protein, respectively). The lower value for the cytochrome c_3 is due to a greater solvent exposure of the hemes.[13] With all these similarities, we are expecting comparable spectral properties for these two assemblies. In fact, as reported by O'Connor et al.,[13] the absorption spectra of the ferric, ferrous, and the ferrous-CO forms of the cytochrome c_3, are remarkably similar to the absorptions described in Figure 10. By analogy, we can consider that reduced 2 hemes-$[H10H24]_2$, like cytochrome c_3, ligates CO at the sixth coordination site, with the fifth site still occupied by histidine. Furthermore, the fact that hemes in the SAM bind CO without being desorbed from the film is another indication that the fifth ligand, e.g., histidine, must play the role of anchor for the porphyrin to the peptide, and therefore to the substrate.

Conclusions

The formation of SAMs of de novo hemoprotein maquettes was successfully achieved in two different ways. Initial chemisorption of synthetic apoprotein followed by incorporation of heme produced a film containing together ligated and unligated hemes. Removal of the uncoordinated hemes leads to a monolayer of hemoprotein with all histidine coordination sites occupied. On the other hand, holoproteins preformed in solution lost half their ligated hemes upon formation of SAM, most probably because of steric hindrance between pairs of hemes in near contact at 10 or 24 positions. The newly designed $[H10H24\text{-}L6I,L13F]_2$ is an exception since it can partially maintain the ligation of 75% of the hemes. We have shown that the synthetic hemoproteins can still be considered as maquettes after the formation of SAM: Even if some of the hemes lost their coordination to the histidines, the remaining ligated ones display remarkably similar spectral properties as in solution and, furthermore, they are able in their reduced state to ligate CO reversibly without being removed from the film. It is important to remember that, in contrast with cytochrome c_3, in the synthetic proteins there is no thioether linkage to immobilize the hemes. The only point of anchorage is through the bis-histidyl ligation. Finally, we want to point out two important observations. (1) Reversibility: Most of the processes described in this study show a remarkable reversibility. Incorporation of hemes in SAMs of apoproteins followed by removal of the physisorbed ones can be repeated several times with excellent reproducibility of the absorption spectra. On the other hand, even if the absorption of the SAM of holoproteins decreases by 30% after reduction and ligation to CO, the film can be reduced again and still coordinates CO. (2) Reproducibility: We observed that the formation of SAMs of synthetic proteins show an excellent reproducibility, usually higher than 95%. These last two points are important because they indicate that the SAMs are not only structured, but that one of their constituents, the hemes, occupy specific sites in the film.

These SAMs represent a crucial stage in the development of films that are both robust and able to exploit the sophisticated chemistry of biological systems. These bundles have been designed with extraordinary stability that permits us to change the amino acids sequence at will in ways natural proteins cannot tolerate. We are beginning to explore structure/binding/function relationships that provide insight into the more complex natural systems. As demonstrated with CO, films of synthetic hemoproteins are sensitive to molecules dissolved in aqueous solution and can be of great utility as chemical and biochemical sensors. By carefully choosing the position of the hemes inside the bundles and by immobilizing the whole assembly between electrodes (gold for example), construction of molecular wires with a series of hemes as conducting material and α-helices as insulator can be investigated. This will certainly play an important role in the development of nanotechnology.

Acknowledgment. The support of this work by grants from NIH (GM 41048) and from the Swiss National Fund for the Scientific Research is acknowledged. B.R.G. was supported by GM 17816 (NIH postdoctoral fellowship). We also thank Xiaoxi Chen and Dr. Konda S. Reddy for the many stimulating discussions.

References and Notes

(1) Photosynthetic reaction center from the purple bacterium *Rhodopseudomonas viridis*: Deisenhofer, J.; Michel, H. *Science* **1989**, *245*, 1463−1473. Deisenhofer, J.; Epp, O.; Miki, K.; Huber, R.; Michel, H. *Nature* **1985**, *318*, 618−624. Photosynthetic reaction center from *Rhodobacter sphaeroides*: Yeates, T. O.; Komiya, H.; Chirino, A.; Rees, D. C.; Allen, J. P.; Feher, G. *Proc. Natl. Acad. Sci. U.S.A.*, **1988**, *85*, 7993−7997.

(2) Tsukihara, T.; Aoyama, H.; Yamashita, E.; Tomizaki, T.; Yamaguchi, H.; Shinzawa-Itoh, K.; Nakashima, R.; Yaono, R.; Yoshikawa, S. *Science* **1995**, *269*, 1069−1074.

(3) Xia, D.; Yu C.-A.; Kim, H.; Xia, J.-Z.; Kachurin, A. M.; Zhang, L.; Yu, L.; Deisenhofer, J. *Science* **1997**, *277*, 60−66. Tsukihara, T.;

Aoyama, H.; Yamashita, E.; Tomizaki, T.; Yamaguchi, H.; Shinzawa-Itoh, K.; Nakashima, R.; Yaono, R.; Yoshikawa, S. *Science* **1996**, *272*, 1136−1144.

(4) DeGrado, W. F.; Wasserman, Z. R.; Lear, J. D. *Science* **1989**, *243*, 622−628.

(5) Robertson, D. E.; Farid, R. S.; Moser, C. C.; Urbauer, J. L.; Mulholland, S. E.; Pidikiti, R.; Lear, J. D.; Wand, A. J.; DeGrado, W. F.; Dutton, P. L. *Nature* **1994**, *368*, 425−432.

(6) Rabanal F.; DeGrado, W. F.; Dutton, P. L. *J. Am. Chem. Soc.* **1996**, *118*, 8, 473−474.

(7) Kalsbeck, W. A.; Robertson, D. E.; Pandey, R. K.; Smith, K. M.; Dutton, P. L.; Bocian, D. F. *Biochemistry* **1996**, *35*, 3429.

(8) For an introduction to the techniques: (a) Ulman, A. *An Introduction to Ultrathin organic Films*; Academic Press, San Diego, CA, **1991**. For reviews concerning electrochemistry of surfaces: (b) Anderson, J. L.; Bowden E. F.; Pickup, P. G. *Anal. Chem.* **1996**, *68*, 379R−444R. Surface characterization: (c) McGuire, G. E.; Ray, M. A.; Simko, S. J.; Perkins, F. K.; Brandow, S. L.; Dobisz, E. A.; Nemanich, R. J.; Chourisia, A. R.; Chopra, D. R. *Anal. Chem.* **1993**, *65*, 311R−333R.

(9) Some examples of reviews related to chemical sensors: (a) Optoelectronic systems: Willmer, I.; Willmer, B. *Adv. Mater.* **1997**, *9* (4), 351−355. Miniaturization: (b) Göpel, W. *Sens. Actuators, A* **1996**, *56*, 83−102. A general review: (c) Janata, J.; Josowicz, M.; DeVaney, M. *Anal. Chem.* **1994**, *66*, 207R−228R.

(10) The reviews related to biosensors are too numerous to report all of them. Hereafter, some selected examples are listed. (a) A detailed overview of the principals types of sensors: *Handbook of Biosensors and Electronic Noses*; (Kress-Rogers, E., Ed.; CRC Press: Boca Raton, FL **1997**. (b) Immunosensors: Morgan, C. L.; Newman D. J.; Price C. P. *Clin. Chem.* **1996**, *42 (2)*, 193−209. (c) Description and future: Bergveld, P. *Sens. Actuators, A* **1996**, *56*, 65−73. (d) SAM and enzymes electrodes: Creager, S. E.; Olsen, K. G. *Anal. Chim. Acta* **1995**, *307*, 277−289. (e) Optical sensors: Lübbers, D. W. *Acta Anasthesiol. Scand.* **1995**, *39*, 37−54. (f) In clinical laboratory: Woo, J.; Henry, J. B. H. *Clin. Lab. Med.* **1994**, *14* (3), 459−471.

(11) Netzer, L.; Iscovici, R.; Sagiv, J. *Thin Solid Films* **1983**, *99*, 235−241.

(12) Gibney, B. R.; Rabanal F.; Skalicky, J. J.; Wand, A. J.; Dutton, P. L. *J. Am. Chem. Soc.* **1997**, *119*, 2323−2324.

(13) O'Connor, D. B.; Goldbeck, R. A.; Hazzard, J. H.; Kliger, D. S.; Cusanovich, M. A. *Biophys. J.* **1993**, *65*,1718−1728.

(14) NOCHROMIX solution contains 0.5 M of ammonium persulfate in concentrated sulfuric acid.

(15) Goss, C. A.; Charych, D. H.; Majda, M. *Anal. Chem.* **1991**, *63*, 85−88.

(16) Riddles, P. W.; Blakeley, R. L.; Zerner, B. *Methods Enzymology* **1983**, *91*, 49. Zahler, W. L.; Cleland, W. W. *J. Biol. Chem.* **1968**, *243*, 716−719.

(17) Nuzzo, R. G.; Fusco, F. A.; Allara, D. L. *J. Am. Chem. Soc.* **1987**, *109* (9), 2358.

(18) (a) Gun, J.; Iscovici, R.; Sagiv, J. *J. Colloid Interface Sci.* **1994**, *101*, 201. (b) Iler, R. K. *The Chemistry of Silica;* John Wiley & Sons: New York, 1979; Chapter 6.

(19) Wasserman, S. R.; Whitesides, G. M.; Tidswell, I. M.; Ocko, B. M.; Pershan, P. S.; Axe, J. D. *J. Am. Chem. Soc.* **1989**, *111*, 5852.

(20) Silver, J.; Lukas, B. *Inorg. Chim. Acta* **1983**, *78*, 219−224.

(21) Blasie, J. K.; Erecinska, M.; Sanmuels, S.; Leigh, J. S. *Biochim. Biophys. Acta* **1978**, *501*, 33−52.

(22) Brahms, S.; Brahms, J. *J. Mol. Biol.* **1980**, *138*, 149−178.

(23) (a) Zhou, N. E.; Kay, C. M.; Hodges R. S. *Biochemistry* **1992**, *31*, 5739−5746. (b) Hodges R. S.; Semchuk, P. D.; Taneja, A. K.; Kay, C. M.; Parker, J. M. R.; Mant, C. T. *Pept. Res.* **1988**, *1*, 19−30. (c) Lau, S. Y. M.; Taneja, A. K.; Hodges, R. S. *J. Biol. Chem.* **1984**, *259*, 13253−13261.

(24) (a) Sui, S.-F.; Wu H.; Guo, Y. *J. Biochem.* **1994**, *115*, 1053−1057. (b) de Jongh, H. H. J.; Goormaghtigh, E.; Killian, J. A. *Biochemistry* **1994**, *33* (3), 14521−14528. (c) de Jongh, H. H. J.; Brasseur, R.; Killian, J. A. *Biochemistry* **1994**, *33*, 14529−14535. (d) Wu, Y.; Huang, H. W.; Glenn, A. O. *Biophys. J.* **1990**, *57*, 797−806. (e) Glenn, A. O.; Huang, H. W. *J. Chem. Phys.* **1988**, *89*, 2531−2538. (f) Glenn, A. O.; Huang, H. W. *J. Chem. Phys.* **1988**, *89*, 6956−6962. (g) DeGrado, W. F.; Lear, J. D. *J. Am. Chem. Soc.* **1985**, *107*, 7684−7689. (h) Cornell, D. G. *J. Colloid Interface Sci.* **1978**, *70*, 167−180.

(25) Xiaoxi, C. unpublished results.

(26) Edminston, P. L.; Lee, J. E.; Cheng, S.-S.; Saavedra, S. C. *J. Am. Chem. Soc.* **1997**, *119*, 560−570.

(27) Wood, L. L.; Cheng, S.-S.; Edminston, P. L.; Saavedra, S. C. *J. Am. Chem. Soc.* **1997**, *119*, 571−576.

(28) Adar, F. In *The Porphyrins*; Dolphin, D., Ed.; Academic Press: New York, 1978, p 167−209.

(29) Shifman, J. Unpublished results.

(30) Decatur, S. M.; Boxer, S. G. *Biochem. Biophys. Res. Commun.* **1995**, *212*, 159−164.